

Tolypocladamide H and the Proposed Tolypocladamide NRPS in *Tolypocladium* Species

Richard M. Tehan, Rheannon R. Blount, Ryan L. Goold, Daphne R. Mattos, Nicolas R. Spatafora, Javier F. Tabima, Romina Gazis, Chengshu Wang, Jane E. Ishmael, Joseph W. Spatafora,* and Kerry L. McPhail*



Cite This: *J. Nat. Prod.* 2022, 85, 1363–1373



Read Online

ACCESS |



Metrics & More

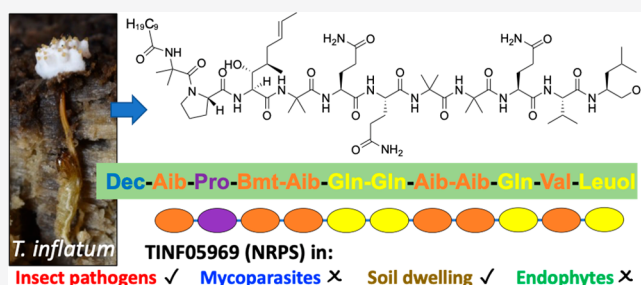


Article Recommendations



Supporting Information

ABSTRACT: The genome of entomopathogenic fungus *Tolypocladium inflatum* Gams encodes 43 putative biosynthetic gene clusters for specialized metabolites, although genotype–phenotype linkages have been reported only for the cyclosporins and fumonisins. *T. inflatum* was cultured in defined minimal media, supplemented with or without one of nine different amino acids. Acquisition of LC-MS/MS data for molecular networking and manual analysis facilitated annotation of putative known and unknown metabolites. These data led us to target a family of peptaibols and guided the isolation and purification of tolypocladamide H (1), which showed modest antibacterial activity and toxicity to mammalian cells at micromolar concentrations. HRMS/MS, NMR, and advanced Marfey's analysis were used to assign the structure of 1 as a peptaibol containing 4-[(*E*)-2-butenyl]-4-methyl-L-threonine (Bmt), a hallmark structural motif of the cyclosporins. LC-MS detection of homologous tolypocladamide metabolites and phylogenomic analyses of peptaibol biosynthetic genes in other cultured *Tolypocladium* species allowed assignment of a putative tolypocladamide nonribosomal peptide synthetase gene.



The diverse fungal genus *Tolypocladium* (Ascomycota, Sodiariomycetes, Hypocreales) is associated with hosts from three kingdoms of life, comprising filamentous species that are foliar or wood endophytes, parasites of other fungi (mycoparasites) and lichens, and pathogens of animals, especially insects.¹ Related to this ecological diversity, *Tolypocladium* and other hypocrealean fungi are prolific producers of biologically active compounds, the majority of which are products of nonribosomal peptides synthetases (NRPS) and polyketide synthases (PKS), with their associated pathways.² *T. inflatum* is a pathogen of beetle larvae that can live as a saprotroph in soil during the asexual phase of its lifestyle and is best known for its production of the immunosuppressant cyclosporins,^{3–5} NRPS-encoded cyclic peptides. *T. inflatum* is readily cultured in the laboratory, and valine supplementation of culture media has been used to increase production of cyclosporin A.^{6,7} Despite harboring 43 putative specialized metabolite biosynthetic gene clusters (BGCs), only a handful of natural products have been reported from *T. inflatum*,^{8–13} and only the peptidic cyclosporins^{14,15} and polyketidic fumonisins¹⁶ have been linked to their corresponding BGCs. *T. inflatum* natural products include peptaibiotics, such as the efrapeptins^{9,10} and closely related tolypins,¹⁷ which are nonribosomal linear peptides characterized by the presence of alpha-amino

isobutyric acid (Aib) and various other nonproteinogenic amino acids. The N-terminus of peptaibiotics is usually acylated with a fatty acid moiety, and peptaibols additionally contain an amino alcohol residue on the C-terminus. To date, *Tolypocladium* species are known to produce peptaibiotics comprising 11 residues (LP237-F5, -F7, and -F8,^{18,19} dakwaabakains A–E²⁰), 16 residues (efrapeptins^{9,10,21}), and 22 residues (gichigamins²⁰). These membrane-active metabolites often possess antimicrobial and cancer cytotoxic properties and are also well known from mycoparasitic fungi.²²

We investigated the metabolome of genome-sequenced *Tolypocladium inflatum* NRRL 8044 in laboratory culture as part of a larger study to define ecological patterns of specialized metabolite biosynthetic gene evolution.²³ In the current study, an approach using variable amino acid supplementation of a defined minimal culture medium induced differential patterns of specialized metabolite production by *T. inflatum* mycelium. The resultant distinct metabolome of valine-supplemented

Received: February 14, 2022

Published: May 2, 2022



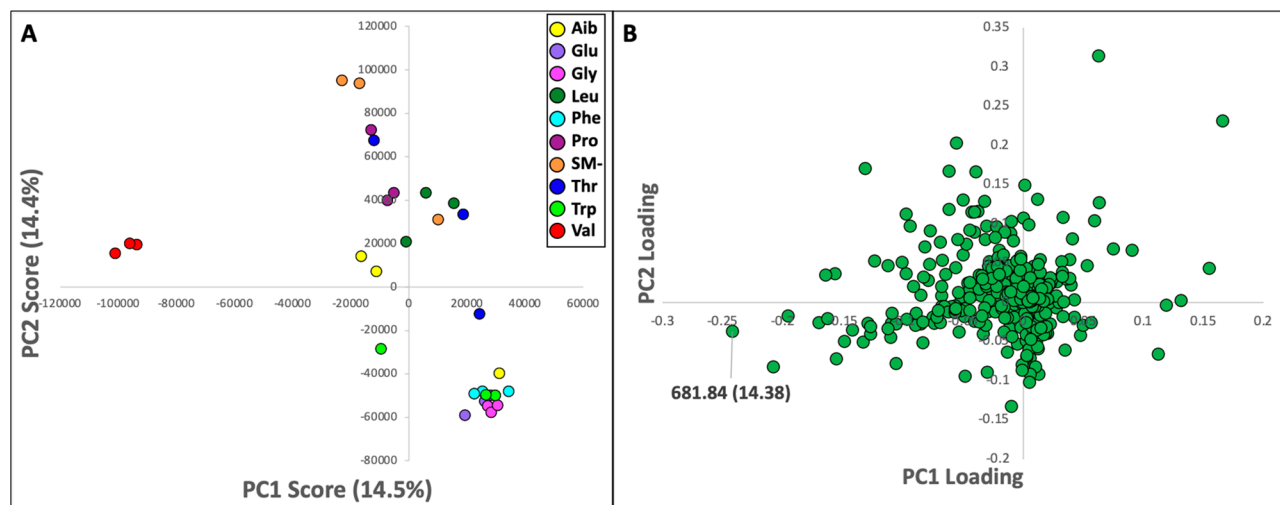


Figure 1. Principal component analysis of extracts of cultured *T. inflatum*. (A) PCA plot of LC-MS data for extracts of *T. inflatum* cultured in triplicate on 10 different defined media (SM), each supplemented with one of nine amino acids (e.g., SM-Val, in red) or not (SM-, in orange). (B) Plot of mass feature loadings for principal components 1 and 2, with the $[M + 2H]^{2+}$ ion for tolypocladamide H (**1**), found in SM-Val isolates, labeled with precursor mass and retention time.

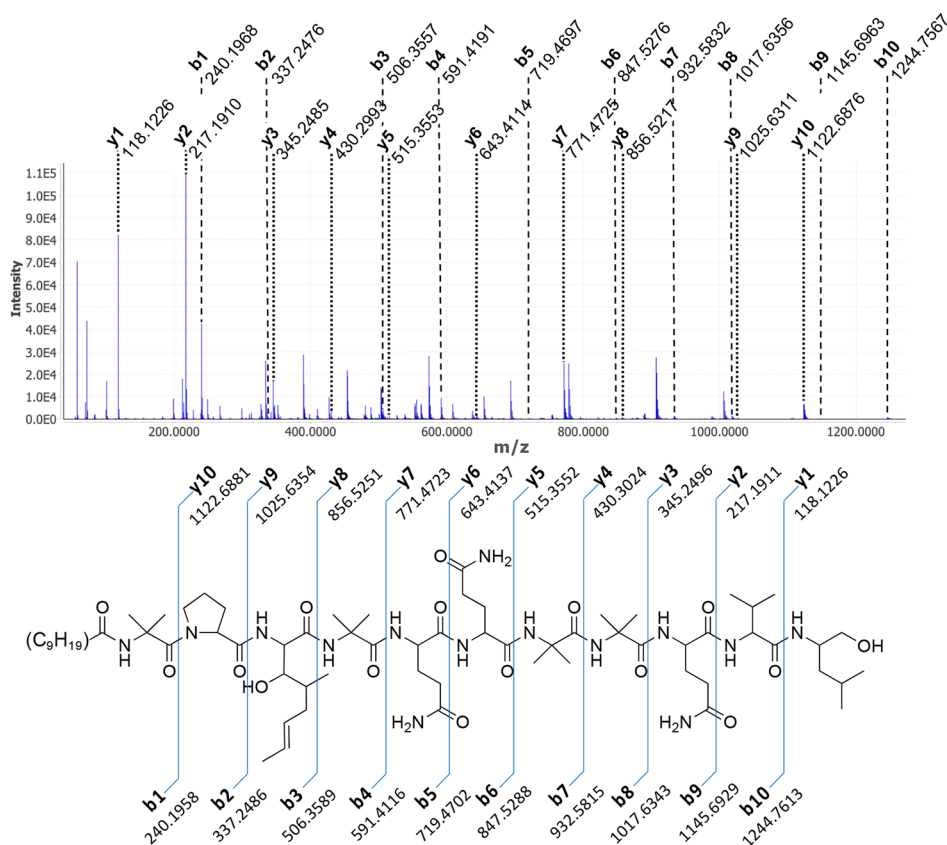


Figure 2. Collision-induced dissociation (CID) qTOF MS-MS spectrum of tolypocladamide H (**1**), with b- and y-type ions labeled, and the planar structure of **1**, with predicted b- and y-type fragments.

cultures was selected for further investigation and led to characterization of tolypocladamide H (**1**), one member of a new series of 11-mer lipopeptaibols (Senadeera et al.²⁴). Our linkage of this molecular family to an 11-module NRPS gene is based on LC-MS detection of structurally similar, yet variable length, lipopeptaibols from other cultured *Tolyopocladium* species, in concert with comparison of candidate NRPS genes across these genome-sequenced species.

RESULTS AND DISCUSSION

In a study designed to induce differential expression of secondary metabolites, the entomopathogenic fungus *Tolyopocladium inflatum* NRRL 8044 was cultured in triplicate on a defined minimal medium (SM) that was either supplemented with one of nine different amino acids or not (SM-), representing 10 culture conditions. Half of the tissue from each of the 33 separate cultures was taken for chemical extraction

Table 1. ¹H (800 MHz) and ¹³C (200 MHz) NMR Data for Tolyocladamide H (1) in MeOD-d₄

unit	position	δ _C ^a type	δ _H , mult (J in Hz)	unit	position	δ _C ^a type	δ _H , mult (J in Hz)
N-Dc-Aib-1	1	175.0, C			5-NH ₂		^b
	2	57.7, C			NH		7.69, d (8)
	3	26.97, CH ₃	1.53, s	L-Gln-6	1	177.2, C	
	4	23.5, CH ₃	1.49, s		2	57.2, CH	4.09, t (7.7)
	NH		^b		3	27.4, CH ₂	2.16, m
	1'	176.5, C			4	32.5, CH ₂	2.35, m
	2'	36.3, CH ₂	2.38, m		5	175.2, C	
			2.34, m		5-NH ₂		^b
	3'	26.6, CH ₂	1.66, obs		NH		^b
	4'	30.3, CH ₂	1.35, obs		Aib-7	1	177.2, C
5'	30.4, CH ₂	1.31, obs	2			57.8, C	
6'	30.4, CH ₂	1.31, obs	3			27.1, CH ₃	1.526, s
7'	30.4, CH ₂	1.31, obs	4	23.4, CH ₃	1.46, s		
8'	33.0, CH ₂	1.29, obs	NH		^b		
9'	26.6, CH ₂	1.32, obs	Aib-8	1	178.5, C		
10'	14.4, CH ₃	0.894, obs		2	57.8, C		
L-Pro-2	1	176.2, C		3	27.0, CH ₃	1.533, s	
	2	64.8, CH	4.49, t (8.1)	4	23.5, CH ₃	1.50, s	
	3	29.9, CH ₂	2.39, obs	NH		7.71, s	
			1.77 dq (15.7, 7.7)	L-Gln-9	1	175.4, C	
	4	27.0, CH ₂	2.01, m		2	56.9, CH	4.02, obs
5	49.9, CH ₂	3.90, ddd (10.9, 6.7, 4.3)	3		28.0, CH ₂	2.22, m	
		3.48, m	4		33.2, CH ₂	2.59, m	
Bmt-3	1	174.2, C			5	177.5, C	
	2	59.8, CH	4.34, d (4.2)	5-NH ₂		^b	
	3	76.0, CH	3.80, dd (8.5, 4.2)	NH		7.84, d (5.6)	
	4	37.8, CH	1.61, m	L-Val-10	1	173.9, C	
	5	36.2, CH ₂	2.48, obs		2	56.9, CH	4.05, obs
			1.92, dt (13.8, 8.6)		3	31.1, CH	2.24, obs
	6	130.0, CH	5.41, dt (13.1, 6.8)		4	19.8, CH ₃	1.06, d (6.7)
	7	127.9, CH	5.49, dq (13.1, 6.4)		5	19.7, CH ₃	1.00, d (6.8)
	8	18.2, CH ₃	1.66, d (6.4)	NH		^b	
	4'	15.8, CH ₃	0.84, d (6.8)	L-Leuol-11	1	50.7, CH	4.04, obs
NH		^b	2		40.6, CH ₂	1.53, obs	
OH		^b			3	25.6, CH	1.71, m
Aib-4	1	178.0, C		4	21.8, CH ₃	0.897, obs	
	2	58.2, C		5	23.9, CH ₃	0.91, obs	
	3	27.2, CH ₃	1.60, s	6	65.8, CH ₂	3.51, obs	
	4	24.0, CH ₃	1.51, s	NH		7.25, d (9.0)	
	NH		^b	OH		^b	
L-Gln-5	1	177.1, C					
	2	62.4, CH	4.05, obs				
	3	27.4, CH ₂	2.15, m				
	4	32.7, CH ₂	2.41, m				
	5	175.6, C					

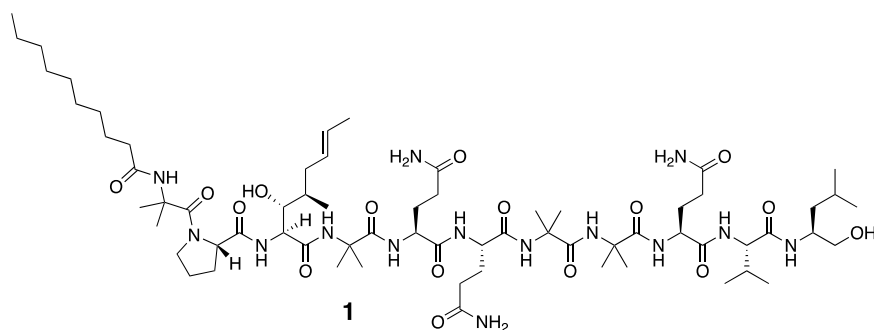
^aValues determined by analysis of HMBC correlations. ^bSignals not detected.

and LC-MS/MS profiling, while the other half was used for RNA extraction and sequencing.²³ The 33 fungal extracts were each prefractionated by RP₁₈ solid phase extraction to produce A1 and A2 fractions, eluted in 50% and 100% MeOH, respectively, for profiling by LC-MS/MS. The A2 fractions consistently yielded a rich spectrum of distinct metabolites, in contrast to the sparse profiles for the A1 fractions. Thus, metabolomic analyses were performed using LC-MS/MS data for A2 fractions only.

Principal component analysis (PCA) of the LC-MS/MS data for chemical extracts of the fungal cultures under investigation revealed significant differences in metabolite production between media conditions. PC1 and PC2 each accounted for greater than 14% of the variance. Extracts of *T.*

inflatum grown in SM-Val grouped separately to extracts of cultures from the other media (Figure 1A). An unknown mass feature with *m/z* 681.8 and retention time 14.4 min was the greatest driver of separation of the SM-Val isolates (Figure 1B).

The mass peak at *m/z* 681.8 could be attributed to the doubly charged ion for a putative peptaibol of molecular mass 1361.5 Da, based on multiple diagnostic losses in its MS/MS spectrum of 85 mass units corresponding to Aib,²⁵ and a mass peak at *m/z* 118 for a reduced C-terminal leucinol (Leuol) or isoleucinol (Ileol). Notably, the doubly charged ion at *m/z* 681.8 for this putative peptaibol was only abundant in the SM-Val cultures, while mass features (e.g., *m/z* 653, 695, 659, 660, 688) with similar fragmentation patterns and retention times



were readily apparent in the LC-MS data acquired for all *T. inflatum* culture conditions. High-resolution MS/MS data confirmed the putative structural class and permitted assignment of amino acid composition and sequence for this suite of related peptaibols, named tolypocladamides, which were elucidated in a similar time frame to those reported by Senadeera et al.²⁴ Specifically, an HRESI(+)-MS ion at m/z 1361.8773 ($[M + H]^+$) for tolypocladamide H (**1**) yielded a molecular formula of $C_{66}H_{116}N_{14}O_{16}$, indicating 16 degrees of unsaturation. Manual assignment of peaks in the HRMS/MS spectrum for **1** delineated a comprehensive series of b- and y-type ions (Figure 2) that revealed a characteristic N-terminal sequence of decanoyl-Aib-Pro, two adjacent Gln residues in mid sequence, multiple Aib residues, and a C-terminal Leuol. Notably, b/y ions did not correspond to the most intense peaks in the MS/MS spectrum for **1**, which were instead readily interpretable as internal b-type ion fragments after an initial loss of the N-terminal fatty acyl moiety and first amino acid residue (Aib-1) (Figure 2, Table S3). This lipopeptaibol framework is akin to that of the three LP-237 peptaibols reported from *T. geodes*^{18,19,26} and dakwaabakains A–E from *Tolyopocladium* sp. Sup5-1, which were isolated alongside LP-237-F7.²⁰ Two points of difference in the structure of **1** were evident at the amino acid-3 (AA-3) and AA-10 positions. Tolypocladamide H (**1**) comprises Val-10, in contrast to Ala-10 in the LP-237 peptaibols and Leu-10 in the dakwaabakains. AA-3 is an aromatic amino acid (Phe or Tyr) in the LP-237 peptaibols and dakwaabakains B–E and a Leu in dakwaabakain A. None of these three residues could be assigned to AA-3 in **1** from the MS/MS data. Instead, considering the molecular formula of $C_{66}H_{116}N_{14}O_{16}$ for **1**, AA-3 could be assigned a formula of $C_9H_{15}NO_2$, which accounts for two degrees of unsaturation and a side chain comprising $C_7H_{13}O$.

In order to determine the structure of AA-3 and confirm the MS/MS-predicted structure using NMR, tolypocladamide H (**1**) was purified from cultures of the *T. inflatum simA* knockout mutant.¹⁵ Use of this mutant strain facilitated purification of **1**, in the absence of cyclosporins, for acquisition of NMR data in DMSO- d_6 and MeOD- d_4 at 600 and 800 MHz and for assignment of chiral amino acid configurations using advanced Marfey's analysis.²⁷ The MeOD- d_4 NMR data are discussed here since these data were acquired at higher field on a greater amount of material and are complementary to those presented by Senadeera et al.²⁴ The 1H NMR spectrum for **1** exhibited chemical shifts typical for a peptidic metabolite, including exchangeable NH signals (δ_H 7.25–8.10), α -H multiplets (δ_H 4.02–4.49), and numerous methyl doublets (δ_H 0.84–1.66, Table 1), together with broad signals in the methylene envelope (δ_H 1.25–1.40). Notably, the presence of multiple methyl singlets (δ_H 1.46–1.60) was consistent with the expected Aib moieties. Additionally, a coupled pair of

deshielded methine 1H signals (δ_H 5.42, 5.49) were consistent with an olefin in an alkyl chain (Figure S1). Given the absence of an olefin in the proposed MS-based structure, it could be assumed that the latter olefin signals originated from the unassigned side chain ($C_7H_{13}O$) for the AA-3 residue. In the COSY spectrum (Figure S2), the olefinic signal at δ_H 5.49 (δ_C 127.9, CH-7) was correlated only to an obscured methyl doublet at δ_H 1.66 (H₃₋₈), while the olefinic signal δ_H 5.42 (δ_C 130.1, CH-6) exhibited correlations to signals for diastereotopic methylene protons at δ_H 2.48 and 1.92 (H₂₋₅), which enabled further delineation of the AA-3 spin system. In particular, the signal at δ_H 1.92 was correlated to a methine at δ_H 1.62 (H-4), which in turn was coupled to a methyl doublet at δ_H 0.84 (H_{3-4'}) as well as a deshielded methine at δ_H 3.80 (H-3). Finally, correlation of the latter methine to the α -H signal at δ_H 4.34 completed the spin system of a 2-butenyl-4-methylthreonine (Bmt) residue. NMR analysis also enabled assignment of a C-terminal Leuol, rather than an isobaric Ileol or other moiety. The remaining amino acids assigned from mass data were consistent with the NMR data (Table 1).

The configurations of the amino acid residues in **1** were assigned using the advanced Marfey's reagent L-FDLA²⁷ to derivatize the natural product hydrolysate and amino acid standards, which evinced all L-configurations for canonical chiral residues, Pro, Gln (as Glu),²⁸ Val, and Leuol. These assignments were consistent with the absence of epimerization domains in the proposed parent NRPS. In the absence of authentic Bmt standards, the hydrolysate of **1** was also derivatized with D-FDLA, which together with the L-FDLA derivative, provided two retention times for two pairs of enantiomers²⁷ from which a 2S configuration for Bmt could be inferred. Homo- and heteronuclear coupling constants obtained from 1H NMR and HETLOC spectra for **1** in MeOD- d_4 permitted partial J-based configurational analysis. Taken together, the small coupling constants for $^3J_{H_2-H_3}$ (4 Hz), $^2J_{H_2-C_3}$ (−3 Hz), $^2J_{H_3-C_2}$ (1 Hz), and $^3J_{H_2-C_4}$ (2 Hz) indicated a threo relative configuration for C-2 and C-3 (Figure S6).²⁹ These measurements were further supported by correlations in the DMSO- d_6 ROESY spectrum (Figure S11) between the Bmt 2-NH (δ_H 7.74) and 3-OH (δ_H 4.72), between H-3 (δ_H 3.67) and H-4 (δ_H 1.48), and between H-2 (δ_H 4.15) and H-3. The HETLOC-derived heteronuclear combined with homonuclear coupling constants ($J_{H_3-H_4} = 8.5$ Hz) for **1** in MeOD- d_4 were not definitive for assignment of the relative configuration between C-3 and C-4 (Figure S6). However, in the DMSO- d_6 1H NMR spectrum for **1** (Figure S7, Table S1), a large $J_{H_3-H_4}$ (11.5 Hz) could be deduced from the H-3 multiplet (δ_H 3.67). Despite some evidence for rotation of the Bmt side chain, prominent ROESY correlations between H-2/H_{3-4'} and H-3/H_{3-4'}, but not 3-OH/H_{3-4'}, together with ROESY correlations between 3-OH/H-5 (δ_H

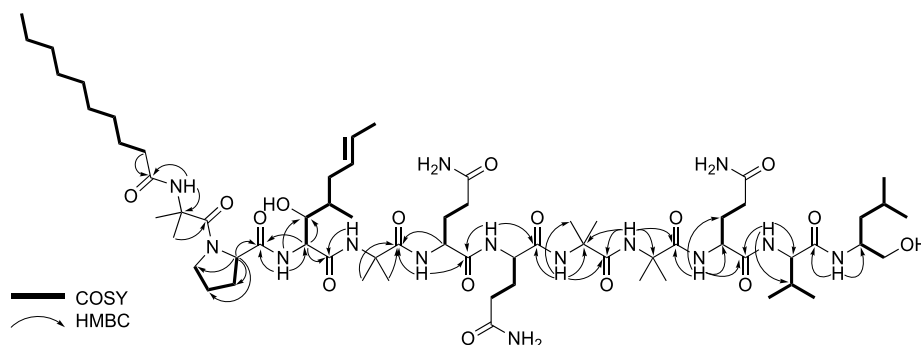


Figure 3. Planar structure of tolypocladamide H (1) showing key COSY and HMBC correlations.

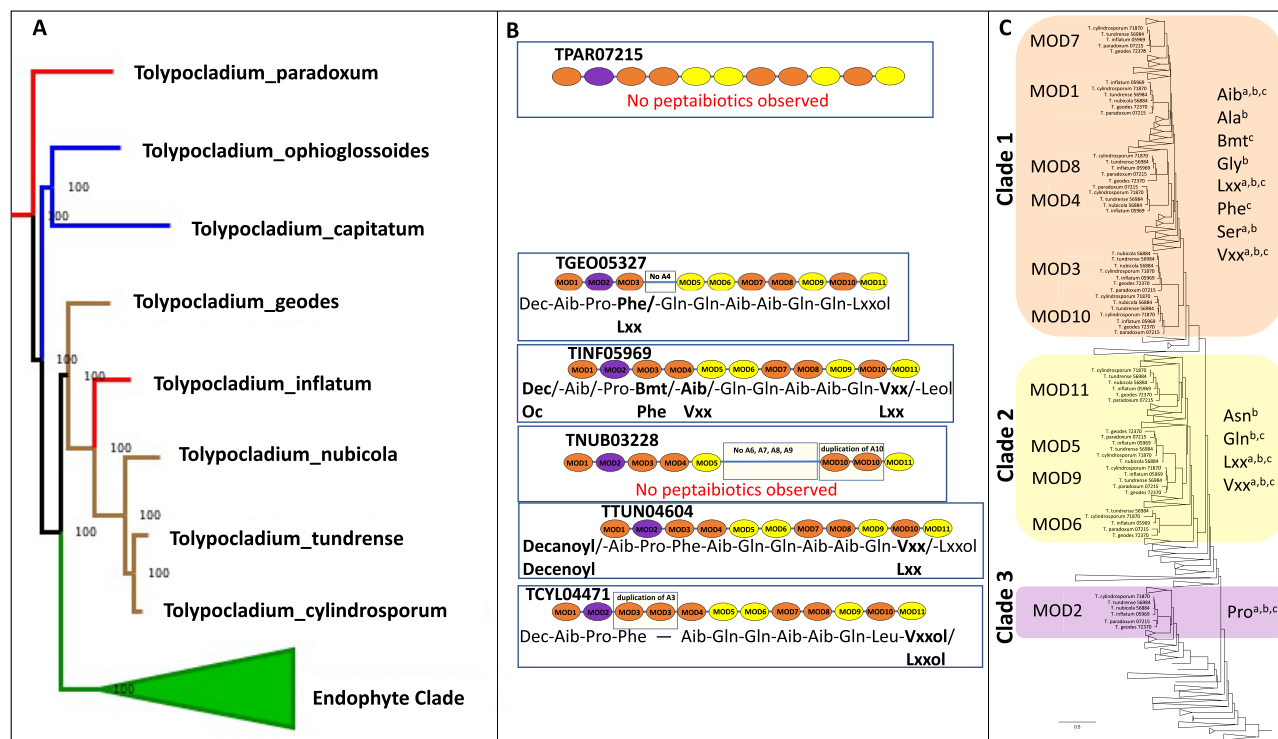


Figure 4. Evolution of tolypocladamides in *Tolypocladium*. (A) Phylogeny of *Tolypocladium* created from 686 single-copy orthologous clusters. Branches are color-coded to ecology (red: insect-associated, blue: mycoparasitic, brown: soil-dwelling, green: endophytic). (B) Representations of the adenylation domains of TINF05969 and TINF05969 homologues, with amino acid sequences of their observed products. Sequence predictions are based on ions observed in MS/MS spectra (Tables S3–S6). A-Domains are color-coded to their respective clade. (C) Phylogeny of peptaibol adenylation domains, with tolypocladamide clades highlighted, and their annotated amino acids listed. ^aReferences 34, 35. ^bReference 35. ^cThis study.

1.79) and H-3/H-5 (δ_{H} 2.36), as well as H-4/3-OH, were consistent with a 4R configuration. An *E* double-bond geometry was indicated by the relatively large olefinic coupling constant ($J_{\text{H}_6-\text{H}_7} = 13$ Hz) and the deshielded chemical shift of the terminal methyl (H_3-8 , δ_{C} 18.2). The assigned (2*S*,3*R*,4*R*,6*E*)-Bmt is consistent with the configuration reported for NMeBmt and Bmt residues in the cyclosporins^{30–32} and is also consistent with the assignments made for Bmt-containing tolypocladamides A–E.²⁴ Tolypocladamide H (1) is most closely related to tolypocladamide E,²⁴ comprising Val-10 in place of Leu-10 in the latter.

Specialized metabolite gene annotation and prediction has identified 656 genes clustered within 43 BGCs in the *T. inflatum* genome. These include 19 NRPS (or “NRPS-like”, by AntiSMASH), 13 PKS, four terpenes, three hybrid NRPS/PKS, and four clusters that included both an NRPS and a

PKS.²³ Three of the NRPS genes are predicted to encode peptaibiotics,^{14,33} and adenylation domains of these modules were the focus of phylogenomic analyses. These candidate tolypocladamide NRPS genes were examined in the context of a phylogeny of 706 adenylation domains constructed previously using an A-domain-specific hidden Markov model created from known fungal A-domains.²³ Known non-peptaibiotic large NRPS A-domains cluster into distinct clades, including the cyclosporin and destruxin clades. Predicted peptaibiotic adenylation domains clustered in three distinct clades (Figure 4, Figure S14).³³ A-Domains from clade 1 are known to activate Aib, Ala, Gly, Ile, Leu, Ser, and Val; clade 2 A-domains are known to activate Asp, Glu, Ile, Leu, and Val; and clade 3 is highly conserved for peptaibiotic A-domains incorporating Pro. Only one *T. inflatum* NRPS (TINF05969) contained 11 A-domains, including one from module 2 in

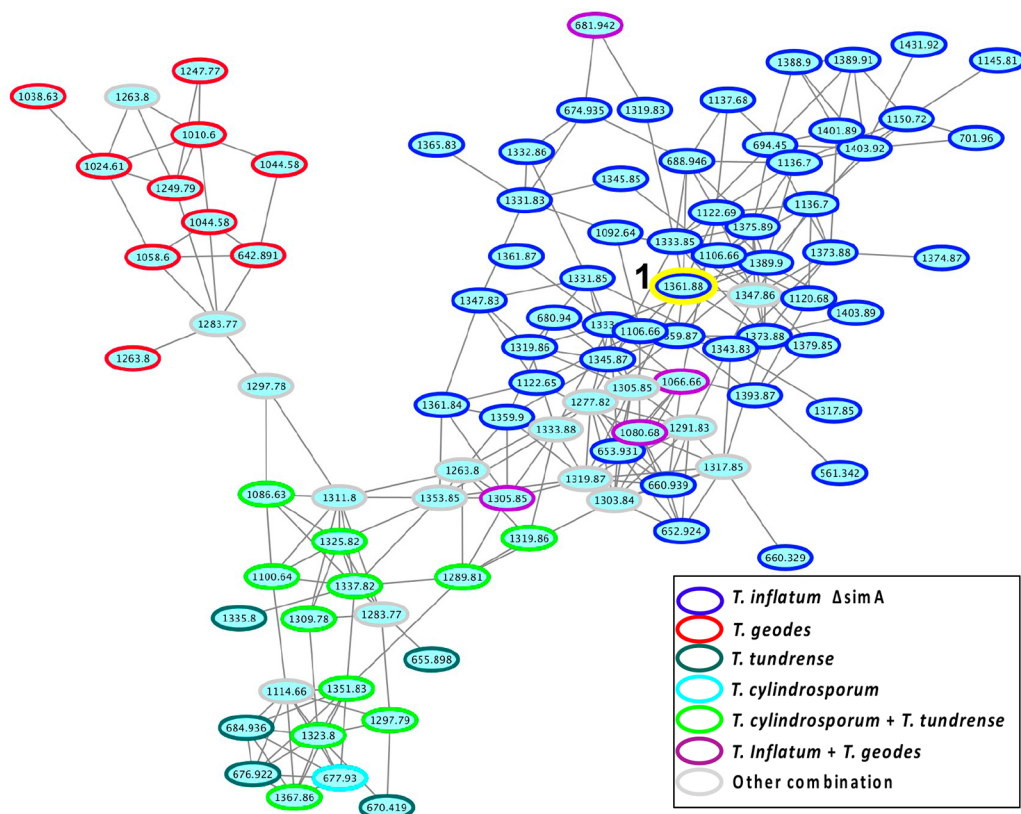


Figure 5. GNPS molecular network of tolypocladamide mass features. Nodes representing mass features in the tolypocladamide molecular family are color-coded by source species of *Tolypocladium*. The mass feature (m/z 1361.88) for tolypocladamide H (**1**) is highlighted in yellow.

peptaibiotic clade 3. The phylogenetically informed A-domain predictions were consistent with the sequence of residues in the tolypocladamide H (**1**) structure assigned from HRMS/MS (Figure 2) and 2D NMR data (Figure 3, Figures S2–S4). For example, module 2 predicts Pro, the second amino acid, and modules 4, 7, and 8 include Aib predictions, the fourth, seventh, and eight amino acid residues of tolypocladamide H (**1**). In total, the 11-module NRPS uses a decanoic acid (Dec) starter unit to produce this 11-residue lipopeptaibol. A-Domain collinearity and phylogeny of TINF05969 are consistent with the amino acid sequence and terminal Val-Leuol of **1**, as well as with other detected tolypocladamide congeners having a terminal Leu-Leuol. These congeners included a tolypocladamide with m/z 1389 and putative sequence DecAib-Pro-Bmt-Aib-Gln-Gln-Aib-Aib-Gln-Leu-Leuol, which is potentially identical to tolypocladamide B, and m/z 1375 (DecAib-Pro-Bmt-Aib-Gln-Gln-Aib-Aib-Gln-Leu-Leuol), which is potentially identical to tolypocladamide F.²⁴ An additional congener with m/z 1348 has a putative sequence of OcAib-Pro-Bmt-Aib-Gln-Gln-Aib-Aib-Gln-Leu/Ile-Leuol/Ileol. All the residues incorporated in observed metabolites were consistent with A-domain phylogeny except for the unusual Bmt residue, not previously observed in any linear peptide natural product. This discovery expands the list of residues known to be accepted by A-domains in clade 1.

TINF05969, identified above as the candidate NRPS for the tolypocladamides, contains A-domains that are homologous (bootstrap value >99) with A-domains of NRPSs from *T. nubicola* (TNUB_03228), *T. cylindrosporim* (TCYL_04471), *T. tundrense* (TTUN_04604), *T. paradoxum* (TPAR_07215), and *T. geodes* (TGEO_05327) (Figure 4). Notably, there is

variation in the number of modules encoded for these NRPSs, and the A-domain phylogeny allows us to identify orthologous domains and which domains were duplicated or deleted, depending on the NRPS (Figure 4B). With these other *Tolypocladium* species in culture, we were able to analyze corresponding LC-MS/MS data for evidence of congeners in the tolypocladamide molecular family. Despite the low relative abundance of b/y ions for these peptaibols, GNPS molecular networking provided a tolypocladamide subnetwork that supported the presence of tolypocladamides in four out of six *Tolypocladium* species investigated (Figure 5). The variation in the number of tolypocladamide NRPS modules was accompanied by a corresponding difference in the number of residues in the tolypocladamide products observed in the four species, as determined by sequencing by MS/MS, providing further evidence for the collinearity of the peptide and the NRPS modules (Figure 4). Whereas *T. inflatum* and *T. tundrense* each have an 11-module NRPS and produce 11-residue peptaibols, *T. geodes* possesses a 10-module NRPS, owing to the loss of module four, and produces 10-residue peptaibols, while *T. cylindrosporim* possesses a 12-module NRPS, owing to the duplication of module three, but the additional module appears to be skipped or not functional^{35,36} and produces 11-residue peptaibols. The putative sequences determined by MS/MS for the peptaibol products from *T. tundrense* (Table S5) and *T. cylindrosporim* (Table S6) exhibit collinearity with the sequences predicted by the adenylation domain phylogeny. Putative tolypocladamide products detected from *T. geodes* possess a Gln-10 in place of a Val/Leu-10 (Figure 4, Table S4), further expanding the amino acids activated by A-domains within clade 1. It is also noteworthy

that the *T. geodes* metabolites are represented as a distinct cluster of mass features in the tolypocladamide subnetwork using standard GNPS molecular networking parameters (Figure 5).

Tolypocladamides display specific phylogenetic and ecological distributions across the genus *Tolypocladium*. Tolypocladamide peptaibols and NRPS genes homologous to TINF05969 are restricted to *T. paradoxum* and species of the *T. inflatum* subclade comprising *T. cylindrosporium*, *T. geodes*, *T. inflatum*, *T. nubicola*, and *T. tundrense*. All of these fungi are known to be either pathogens of soil or wood-inhabiting immature stages of insects or soil-borne fungi.^{1,37} Conversely, tolypocladamide peptides were not detected in, and homologues to TINF05969 were absent from the genomes of, mycoparasites *T. capitatum* and *T. ophioglossoides* and all species isolated as endophytes of plants and lichens (Figure 4, Table S7). This restricted phylogenetic and ecological distribution is suggestive of a role in insect pathogenicity or the soil environment and informs future biological assays and activity screens.

Tolypocladamide H (**1**) was screened for antimicrobial and cytotoxic activity and showed weak to moderate activity against both. Out of a panel of six bacterial and two fungal pathogens, strains with modest susceptibility were *Enterococcus faecium* ATCC BAA-2317 (MIC 16 μ M [22 μ g/mL], linezolid: 89 μ M [30 μ g/mL]) and 8 μ M (11 μ g/mL) for *Staphylococcus aureus* ATCC 25923 (ampicillin: 1.4 μ M [0.5 μ g/mL]). In cancer cytotoxicity assays, tolypocladamide H (**1**) was approximately 1000-fold less cytotoxic to human HeLa cervical (EC₅₀ = 30 μ M) and MCF-7 breast (EC₅₀ = 107 μ M) cancer cells than mitochondrial ATPase inhibitor^{38,39} leucinostatin A (EC₅₀ = 21 and 13 nM, respectively, Figure S15). Comparative analysis of the cytotoxic potential of **1**, leucinostatin A, and cyclosporin A against normal human umbilical vein endothelial cells (HUVECs) also revealed a distinct bioactivity profile. Tolypocladamide H (**1**) induced a concentration-dependent decrease in HUVEC viability (EC₅₀ = 8 μ M), with full efficacy, whereas the relative EC₅₀ of leucinostatin A was <1 μ M. In contrast, the calcineurin inhibitor cyclosporin A was nontoxic at the maximum concentration tested (10 μ M). The modest activity observed for **1** against some Gram-positive bacteria and mammalian cells is consistent with previous observations for peptaibols containing Gln residues, which have been associated with the ability of these peptaibols to form pores in the outer membranes of cells and the tendency to exhibit nonspecific cytotoxicity.⁴⁰

CONCLUSION

Characterization of the molecular structure and production of tolypocladamides across *Tolypocladium* species has provided insight on the ecological patterns of peptide synthetase gene evolution in these Hypocrealean fungi. We propose that 11-residue peptaibols reported from the genus *Tolypocladium*, including the LP237 series,¹⁸ the dakwaabakains,²⁰ and now the tolypocladamides,²⁴ form a biosynthetically related molecular family as products of homologous NRPS genes. Tolypocladamide H and homologues of the NRPS TINF05969 are restricted in their phylogenetic distribution within *Tolypocladium* to known insect pathogens and closely related soil-inhabiting species. Importantly, the peptaibols were not detected and the linked NRPS homologues were absent from mycoparasitic and endophytic species of the genus. Previously, Bmt has only been reported in cyclosporins and, in

that case, is attributed to the Sim G PKS in tandem with cytochrome P450 Sim I and aminotransferase Sim J, which are clustered with the SimA NRPS in the cyclosporin biosynthetic gene cluster.¹⁵ Interestingly, there are two homologues of the Sim G PKS in the *T. inflatum* genome, and further work is needed to determine the biosynthetic source of Bmt in the tolypocladamides, which constitute the first instance of a Bmt residue in a linear peptidic natural product. This unique polyketide motif at AA-3 is accompanied by residues that are otherwise typical of peptaibol natural products, of which there are numerous examples from hypocrealean fungi. A notable comparison can be made to the structural motif encompassed by the 10-residue peptaibiotic leucinostatin A³⁸ and its 9- and 10-residue congeners reviewed by Stubbing et al.,⁴¹ which possess a Pro or 4-methyl-Pro residue followed by an AHMOD (2-amino-6-hydroxy-4-methyl-8-oxodecanoate) residue, near the N-terminus, akin to the Pro-Bmt motif in the tolypocladamides. Both AHMOD and Bmt have linear side chains of PKS origin, with hydroxy and methyl substituents, and both are only known from hypocrealean fungi. Nonetheless, independent origins of this unique structural motif are indicated because the peptide synthetases encoding Bmt- and AHMOD-containing peptaibiotics fall in distinct clades, presenting an interesting instance of convergent evolution in specialized metabolite structure.

EXPERIMENTAL SECTION

General Experimental Procedures. Optical rotation was measured on a JASCO P-1010 polarimeter. NMR spectra were acquired on either a Bruker AVANCE III 800 equipped with a TXI 5 mm cryoprobe at 300 K or a Bruker AVANCE III 600 equipped with a 1.7 mm inverse detection triple resonance (H-C/N/D) cryoprobe at 300 K. NMR spectra were calibrated to residual protonated methanol-*d*₄ (δ_{H} 3.31, δ_{C} 49.15) or to residual protonated DMSO-*d*₆ (δ_{H} 2.50, δ_{C} 39.52). The isolation of compound **1** was performed on a Shimadzu HPLC system equipped with two LC-20AD pumps and an SPD-M20A photodiode array detector. Low-resolution LC-MS/MS data were acquired on an ABSCIEX 3200 QTrap in tandem with a Shimadzu HPLC system. Accurate mass (HRTOFMS, ES⁺) measurements were acquired on an ABSciex TripleTOF 5600 or an Agilent 6545 TOF mass spectrometer. High-resolution LC-MS/MS and Marfey's analyses were conducted on an Agilent 1260 Infinity II LC system with detection by an Agilent 6545 TOF mass spectrometer from *m/z* 100 to 3000. General reagents were from TCI-America, Sigma-Aldrich Corp., and VWR International.

Fungal Laboratory Culture and Tissue Harvest. Cultures of *Tolypocladium inflatum* NRRL 8044 were first grown on potato dextrose agar (PDA, IBI, Dubuque, IA, USA) to create inoculum for future culture experiments. Selective media (for 1 L: 30 g fructose, 10 g (NH₄)₂SO₄, 0.75 g KH₂PO₄, 1.03 g MgSO₄·7H₂O, 0.13 CaCl₂·2H₂O, 1 mL trace element solution [2.2 g ZnSO₄·7H₂O, 0.09 g MnCl₂·4H₂O, 0.0145 g Na₂MoO₄·2H₂O, 0.04 g CuSO₄·5H₂O, 2.5 g FeSO₄·7H₂O, 1 mL H₂SO₄], 6 g/L amino acid mixed separately in 100 mL of dH₂O and sterilized with a syringe filter) were supplemented with different amino acids to induce differential expression of secondary metabolites in *T. inflatum*. Amino acids used in the study were valine (ThermoFisher ACROS Organics, Geel, Belgium), leucine (MP Biomedicals, Santa Ana, CA, USA), proline (MP Biomedicals), aminoisobutyric acid, tryptophan (Alfa Aesar by ThermoFisher Scientific, Tewksbury, MA, USA), phenylalanine (ThermoFisher ACROS Organics), glutamine (ThermoFisher Scientific, Pittsburgh, PA, USA), glycine (ThermoFisher ACROS Organics), threonine (ThermoFisher ACROS Organics), and a final condition that included the base medium without addition of any amino acid (SM-). The protocol for media preparation was altered from Lee et al.⁴²

t_R 16.5–21 min was defatted with a 1:1 hexanes–MeOH partition, and the MeOH fraction was separated by HPLC using a Phenomenex Synergi 4 μ Max (C₁₈) 250 \times 10 mm 80 Å column, with an isocratic mobile phase of 67:33 MeCN + 0.1% FA–H₂O + 0.1% FA. A fraction with t_R 13–17.5 min was collected and further separated using a Phenomenex Kinetex 2.6 μ RP₁₈ 250 \times 10 mm 100 Å column, with an isocratic mobile phase of 64:36 MeCN + 0.1% FA–H₂O + 0.1% FA, to yield tolypocladamide H (1, 1.8 mg).

Tolypocladamide H (1): white solid; $[\alpha]_D^{23}$ –14.0 (c 1.0, MeOH); ¹H and 2D NMR data, see Tables 1 and S1 and the Supporting Information figures; HRTOFMS (ES+) m/z 1361.8773 [M + H]⁺ (calcd for C₆₆H₁₁₇N₁₄O₁₆, 1361.8767).

Absolute Configuration of Tolypocladamide H (1). The absolute configurations of canonical amino acid and amino alcohol residues in 1 were determined using the advanced Marfey's method.²⁷ Compound 1 (175 μ g) was hydrolyzed by refluxing in 6 N HCl at 110 °C for 24 h and concentrated in vacuo, and the hydrolysate was redissolved in H₂O (100 μ L). To this solution was added 1 M NaHCO₃ (40 μ L) followed by 1% (w/v) L-FDLA in acetone (200 μ L). After stirring at 37 °C for 1 h, the reaction was quenched by addition of 1 N HCl (40 μ L) and diluted with MeOH (1.6 mL). An aliquot (1.5 μ L) was analyzed by LC-HRMS using an Agilent Zorbax SB-C3 column, 3.0 \times 250 mm, with a flow rate of 0.4 mL/min and linear gradient from 40:60 MeCN + 0.1% FA–H₂O + 0.1% FA to 60:40 MeCN + 0.1% FA–H₂O + 0.1% FA over 20 min. The absolute configurations of residues were determined by comparison with the retention times of authentic amino acid and amino alcohol standards derivatized with the advanced Marfey's reagent as previously described.²⁷ Due to the hydrolysis of the amide group in Gln residues to a carboxylic acid and ammonia,⁶³ authentic standards of Glu were used to determine the configuration of Gln residues. Additionally, a Gln standard (100 μ g) was hydrolyzed using the hydrolysis conditions above to demonstrate its transformation to Glu. The retention times for advanced Marfey's reagent-derivatized amino acid and amino alcohol standards (min) were as follows: L-Gln (6.7), D-Gln (7.1), L-Glu (8.0), D-Glu (8.8), L-Leuol (16.3), D-Leuol (22.1), L-Pro (9.9), D-Pro (11.7), L-Val (13.1), D-Val (18.3). The retention times for the acid hydrolysate of (1) (min) were as follows: L-Glu (8.0), L-Leuol (16.3), L-Pro (9.9), L-Val (13.1).

For assignment of the Bmt residue, an additional aliquot (175 μ g) of 1 was hydrolyzed as above and derivatized with D-FDLA. The retention times for the L- and D-FDLA derivatives of Bmt in the natural product hydrolysate were 17.9 (2S,3S) and 27.6 min, respectively.

Biological Activity Testing. Tolypocladamide H (1) was screened for antimicrobial activity against a panel of priority pathogens (World Health Organization) that included six strains of bacteria (positive control): *Acinetobacter baumannii* American Type Culture Collection (ATCC) BAA-1605 (amikacin), *Escherichia coli* ATCC BAA-2523 (ciprofloxacin), *Enterococcus faecium* ATCC BAA-2317 (linezolid), *Klebsiella pneumoniae* ATCC BAA-2344 (tetracycline), *Pseudomonas aeruginosa* ATCC BAA-9027 (ciprofloxacin), and *Staphylococcus aureus* ATCC 700698 (vancomycin) and two strains of fungi: *Candida albicans* ATCC MYA-574 (casprofungin) and *Cryptococcus neoformans* ATCC 90112 (fluconazole). Strains were grown in culture tubes (37 °C with shaking at 225 rpm) in 3 mL of media, chosen according to the ATCC recommendation for each respective strain. After incubation for 3–8 h, the cultures were back-diluted to an optical density corresponding to 10⁶ cfu/mL, dispensed into 384-well microtiter plates, and incubated in triplicate with tolypocladamide H (1) at 10 μ M, alongside the positive controls indicated. The DMSO solvent vehicle was used as a negative control. Minimum inhibitory concentration values for 1 were obtained against *Enterococcus faecium* ATCC BAA-2317 (linezolid MIC: 89 μ M [30 μ g/mL]) and *Staphylococcus aureus* ATCC 25923 (ampicillin MIC: 1.4 μ M [0.5 μ g/mL]) by culturing the strains as above and incubating each in triplicate in a 384-well microtiter plate with a dilution series of 1, together with the respective controls.

The cytotoxic potential of tolypocladamide H (1) was assessed against primary human endothelial cells and two human cancer cell

types. For these studies, HUVECs were purchased from Life Technologies (Carlsbad, CA, USA; lot #2363542), expanded and maintained for a limited number of passages in medium 200PRF supplemented with low serum growth supplement (Life Technologies). Human HeLa cervical cancer cells and human MCF-7 breast cancer cells were purchased from ATCC and maintained in minimum essential medium (MEM) with Earl's salts and L-glutamine (Corning Life Sciences, NY, USA) supplemented with 10% fetal bovine serum and 1% penicillin/streptomycin. Leucinostatin A (#76600-38-9) was obtained from BOC Sciences; lapatinib (#SML2259) and cyclosporin A (#C3662) were purchased from Millipore-Sigma. Compounds were reconstituted in 100% DMSO and stored at –20 °C until the day of treatment; final concentrations never exceeded 0.1% DMSO. For viability assays, cells were seeded into 96-well white-wall plates at densities of 5000 cells/well for HUVECs, 2000 cells/well for HeLa cells, and 3000 cells/well for MCF-7 cells. After 18 h, cells were treated at the concentrations indicated for 72 h. Cell viability was assessed at the end of treatment using a CellTiter-Glo luminescent cell viability assay (#G7572; Promega Corp., Madison, WI, USA) using a multimode microplate reader. The viability of vehicle-treated cells was defined as 100% in all studies. Concentration–response relationships were analyzed using GraphPad Prism software version 9.0.0 (GraphPad Software Inc., San Diego, CA, USA), and EC₅₀ values derived using nonlinear regression analysis fit to a logistic equation.

■ ASSOCIATED CONTENT

SI Supporting Information

The Supporting Information is available free of charge at <https://pubs.acs.org/doi/10.1021/acs.jnatprod.2c00153>.

1D and 2D NMR spectra in MeOD-*d*₄ and DMSO-*d*₆; ion chromatograms for advanced Marfey's analysis; graphs and table of cytotoxicity data; complete phylogeny of adenylation domains in hypocrealean fungi; table of ¹H and ¹³C NMR shifts in DMSO-*d*₆ for 1; tables of mass fragment ions for tolypocladamide congeners detected in cultured *Tolypocladium* species; *Tolypocladium* isolate information and genome accession numbers; table of HMM orthologous clusters for Hypocreales genome-scale species phylogeny (PDF)

■ AUTHOR INFORMATION

Corresponding Authors

Kerry L. McPhail – Department of Pharmaceutical Sciences, College of Pharmacy, Oregon State University, Corvallis, Oregon 97331, United States; orcid.org/0000-0003-2076-1002; Phone: +1 541 737 5808; Email: kerry.mcphail@oregonstate.edu

Joseph W. Spatafora – Department of Botany and Plant Pathology, College of Agricultural and Life Sciences, Oregon State University, Corvallis, Oregon 97331, United States; Phone: +1 541 737 8134; Email: joseph.spatafora@oregonstate.edu

Authors

Richard M. Tehan – Department of Pharmaceutical Sciences, College of Pharmacy, Oregon State University, Corvallis, Oregon 97331, United States

Rheannon R. Blount – Department of Botany and Plant Pathology, College of Agricultural and Life Sciences, Oregon State University, Corvallis, Oregon 97331, United States

Ryan L. Goold – Department of Botany and Plant Pathology, College of Agricultural and Life Sciences, Oregon State University, Corvallis, Oregon 97331, United States

Daphne R. Mattos – Department of Pharmaceutical Sciences, College of Pharmacy, Oregon State University, Corvallis, Oregon 97331, United States

Nicolas R. Spatafora – Department of Botany and Plant Pathology, College of Agricultural and Life Sciences, Oregon State University, Corvallis, Oregon 97331, United States

Javier F. Tabima – Department of Botany and Plant Pathology, College of Agricultural and Life Sciences, Oregon State University, Corvallis, Oregon 97331, United States; Department of Biology, Clark University, Worcester, Massachusetts 01610, United States

Romina Gazis – Department of Plant Pathology, Tropical Research and Education Center, University of Florida, Homestead, Florida 33031, United States

Chengshu Wang – Key Laboratory of Insect Developmental and Evolutionary Biology, CAS Center for Excellence in Molecular Plant Sciences, Shanghai Institute of Plant Physiology and Ecology, Chinese Academy of Sciences, Shanghai 200032, People's Republic of China; orcid.org/0000-0003-1477-1466

Jane E. Ishmael – Department of Pharmaceutical Sciences, College of Pharmacy, Oregon State University, Corvallis, Oregon 97331, United States; orcid.org/0000-0003-4574-2801

Complete contact information is available at:

<https://pubs.acs.org/10.1021/acs.jnatprod.2c00153>

Notes

The authors declare no competing financial interest.

ACKNOWLEDGMENTS

This research was supported in part by the National Science Foundation DEB1354944 and by the National Institutes of Health via NIGMS 1R01GM132649 and NCCIH T32 AT010131 (support of R.M.T. and D.R.M.). We acknowledge the support of the Oregon State University NMR Facility funded in part by the National Institutes of Health, HEI Grant 1S10OD018518, and by the M. J. Murdock Charitable Trust Grant 2014162. We thank Mark Dasenko and Chris Sullivan of the OSU Center for Quantitative Life Sciences (CQLS) for sequencing and computational assistance, respectively.

REFERENCES

- (1) Sung, G.-H.; Hywel-Jones, N. L.; Sung, J.-M.; Luangsa-Ard, J. J.; Shrestha, B.; Spatafora, J. W. *Stud. Mycol* **2007**, *57*, 5–59.
- (2) Zhang, L.; Yue, Q.; Wang, C.; Xu, Y.; Molnár, I. *Nat. Prod. Rep* **2020**, *37*, 1164–1180.
- (3) Rüegger, A.; Kuhn, M.; Lichti, H.; Loosli, H. R.; Huguenin, R.; Quiquerez, C.; von Wartburg, A. *Helv. Chim. Acta* **1976**, *59*, 1075–1092.
- (4) Laupacis, A.; Keown, P. A.; Ulan, R. A.; McKenzie, N.; Stiller, C. R. *Can. Med. Assoc. J.* **1982**, *126*, 1041–1046.
- (5) Survase, S. A.; Kagliwal, L. D.; Annapure, U. S.; Singhal, R. S. *Biotechnol. Adv.* **2011**, *29*, 418–435.
- (6) Lee, J.; Agathos, S. N. *Biotechnol. Lett.* **1989**, *11*, 77–82.
- (7) Survase, S. A.; Annapure, U. S.; Singhal, R. S. T. *Curr. Trends Biotechnol. Pharm.* **2010**, *4*, 764–773.
- (8) Bullough, D. A.; Jackson, C. G.; Henderson, P. J. F.; Beechey, R. B.; Linnett, P. E. *FEBS Lett.* **1982**, *145*, 258–262.
- (9) Gupta, S.; Krasnoff, S. B.; Roberts, D. W.; Renwick, J. A. A.; Brinen, L. S.; Clardy, J. *J. Am. Chem. Soc.* **1991**, *113*, 707–709.
- (10) Gupta, S.; Krasnoff, S. B.; Roberts, D. W.; Renwick, J. A. A.; Brinen, L. S.; Clardy, J. *J. Org. Chem.* **1992**, *57*, 2306–2313.

(11) Lin, J.; Chen, X.; Cai, X.; Yu, X.; Liu, X.; Cao, Y.; Che, Y. *J. Nat. Prod* **2011**, *74*, 1798–1804.

(12) Gräfe, U.; Ihn, W.; Schlegel, B.; Höfle, G.; Augustiniak, H.; Sandor, P. *Pharmazie* **1991**, *46*, 613–614.

(13) Gräfe, U.; Ihn, W.; Tresselt, D.; Miosga, N.; Kaden, U.; Schlegel, B.; Bormann, E.-J.; Sedmera, P.; Novák, J. *Biol. Met* **1990**, *3*, 39–44.

(14) Bushley, K. E.; Raja, R.; Jaiswal, P.; Cumbie, J. S.; Nonogaki, M.; Boyd, A. E.; Owensby, C. A.; Knaus, B. J.; Elser, J.; Miller, D.; Di, Y.; McPhail, K. L.; Spatafora, J. W. *PLoS Genet* **2013**, *9*, e1003496.

(15) Yang, X.; Feng, P.; Yin, Y.; Bushley, K.; Spatafora, J. W.; Wang, C. *MBio* **2018**, *9*, e01211–18.

(16) Mogensen, J. M.; Møller, K. A.; von Freiesleben, P.; Labuda, R.; Varga, E.; Sulyok, M.; Kubátová, A.; Thrane, U.; Andersen, B.; Nielsen, K. F. *J. Ind. Microbiol. Biotechnol* **2011**, *38*, 1329–1335.

(17) Brückner, H.; Degenkolb, T. *Chem. Biodivers* **2020**, *17*, e2000276.

(18) Tsantrizos, Y. S.; Pischos, S.; Sauriol, F.; Widden, P. *Can. J. Chem.* **1996**, *74*, 165–172.

(19) Rainaldi, M.; Moretto, A.; Peggion, C.; Formaggio, F.; Mammi, S.; Peggion, E.; Galvez, J. A.; Diaz-de-Villegas, M. D.; Cativiela, C.; Toniolo, C. *Chemistry* **2003**, *9*, 3567–3576.

(20) Du, L.; Risinger, A. L.; Mitchell, C. A.; You, J.; Stamps, B. W.; Pan, N.; King, J. B.; Bopassa, J. C.; Judge, S. I. V.; Yang, Z.; Stevenson, B. S.; Cichewicz, R. H. *Proc. Natl. Acad. Sci. U. S. A* **2017**, *114*, E8957–E8966.

(21) Krasnoff, S. B.; Gupta, S.; Leger, R. J. S.; Renwick, J. A. A.; Roberts, D. W. *J. Invertebr. Pathol* **1991**, *58*, 180–188.

(22) Mukherjee, P. K.; Horwitz, B. A.; Kenerley, C. M. *Microbiol* **2012**, *158*, 35–45.

(23) Blount, R. R. Secondary Metabolism in *Tolypocladium*: Characterization, Ecology, Evolution and Regulation. Ph.D. Dissertation, Oregon State University, Corvallis, OR, 2018.

(24) Senadeera, S. P. D.; Wang, D.; Kim, C.-K.; Smith, E. A.; Henrich, C. J.; Durrant, D. E.; Alexander, P. A.; Morrison, D.; Wendt, K. L.; Cichewicz, R. H.; Beutler, J. A. Tolypocladamides A-G: Bioactive Peptaibols from the Fungus *Tolypocladium Inflatum*.

(25) Degenkolb, T.; Berg, A.; Gams, W.; Schlegel, B.; Gräfe, U. *J. Pept. Sci.* **2003**, *9*, 666–678.

(26) Tsantrizos, Y. S.; Pischos, S.; Sauriol, F. *J. Org. Chem.* **1996**, *61*, 2118–2121.

(27) Fujii, K.; Ikai, Y.; Mayumi, T.; Oka, H.; Suzuki, M.; Harada, K.-I. *Anal. Chem.* **1997**, *69*, 3346–3352.

(28) Rivera-Chávez, J.; Raja, H. A.; Graf, T. N.; Gallagher, J. M.; Metri, P.; Xue, D.; Pearce, C. J.; Oberlies, N. H. *RSC Adv.* **2017**, *7*, 45733–45751.

(29) Matsumori, N.; Kaneno, D.; Murata, M.; Nakamura, H.; Tachibana, K. *J. Org. Chem.* **1999**, *64*, 866–876.

(30) Petcher, T. J.; Weber, H.; Rüegger, A. *Helv. Chim. Acta* **1976**, *59*, 1480–1489.

(31) Traber, R.; Hofmann, H.; Loosli, H. R.; Ponelle, M.; Von Wartburg, A. *Helv. Chim. Acta* **1987**, *70*, 13–36.

(32) Offenzeller, M.; Su, Z.; Santer, G.; Moser, H.; Traber, R.; Memmert, K. *J. Biol. Chem.* **1993**, *268*, 26127–26134.

(33) Quandt, C. A.; Bushley, K. E.; Spatafora, J. W. *BMC Genomics* **2015**, *16*, 553.

(34) Degenkolb, T.; Karimi Aghcheh, R.; Dieckmann, R.; Neuhof, T.; Baker, S. E.; Druzhinina, I. S.; Kubicek, C. P.; Brückner, H.; von Döhren, H. *Chem. Biodivers* **2012**, *9*, 499–535.

(35) Wiest, A.; Grzegorski, D.; Xu, B.-W.; Goulard, C.; Rebuffat, S.; Ebbole, D. J.; Bodo, B.; Kenerley, C. *J. Biol. Chem.* **2002**, *277*, 20862–20868.

(36) Mukherjee, P. K.; Wiest, A.; Ruiz, N.; Keightley, A.; Moran-Diez, M. E.; McCluskey, K.; Pouchus, Y. F.; Kenerley, C. M. *J. Biol. Chem.* **2011**, *286*, 4544–4554.

(37) Gazis, R.; Skaltsas, D.; Chaverri, P. *Mycologia* **2014**, *106*, 1090–1105.

(38) Fukushima, K.; Arai, T.; Mori, Y.; Tsuboi, M.; Suzuki, M. *J. Antibiot.* **1983**, *36*, 1606–1612.

- (39) Momose, I.; Onodera, T.; Doi, H.; Adachi, H.; Iijima, M.; Yamazaki, Y.; Sawa, R.; Kubota, Y.; Igarashi, M.; Kawada, M. *J. Nat. Prod.* **2019**, *82*, 1120–1127.
- (40) de la Fuente-Nunez, C.; Whitmore, L.; Wallace, B. A. In *Handbook of Biologically Active Peptides*; Kastin, A. J., Ed.; Elsevier Academic Press, 2013; pp 150–156.
- (41) Stubbing, L. A.; Kaviani, I.; Brimble, M. A. *Org. Biomol. Chem.* **2017**, *15*, 3542–3549.
- (42) Lee, M.-J.; Lee, H.-N.; Han, K.; Kim, E.-S. *J. Microbiol. Biotechnol.* **2008**, *18*, 913–917.
- (43) Quandt, C. A.; Di, Y.; Elser, J.; Jaiswal, P.; Spatafora, J. W. *G3* **2016**, *6*, 731–741.
- (44) Jiang, H.; Lei, R.; Ding, S.-W.; Zhu, S. *BMC Bioinform.* **2014**, *15*, 182.
- (45) Gordon, A.; Hannon, G. J. FASTX-Toolkit. FASTQ/A Short-Reads Preprocessing Tools. Computer program distributed by the author, 2011.
- (46) Gordon, A.; Hannon, G. J.; et al. Fastx-Toolkit. FASTQ/A short-reads preprocessing tools (unpublished); http://hannonlab.cshl.edu/fastx_toolkit, 2010, 5.
- (47) Zerbino, D. R.; Birney, E. *Genome Res.* **2008**, *18*, 821–829.
- (48) Grabherr, M. G.; Haas, B. J.; Yassour, M.; Levin, J. Z.; Thompson, D. A.; Amit, I.; Adiconis, X.; Fan, L.; Raychowdhury, R.; Zeng, Q.; Chen, Z.; Mauceli, E.; Hacohen, N.; Gnirke, A.; Rhind, N.; di Palma, F.; Birren, B. W.; Nusbaum, C.; Lindblad-Toh, K.; Friedman, N.; Regev, A. *Nat. Biotechnol.* **2011**, *29*, 644–652.
- (49) Cantarel, B. L.; Korf, I.; Robb, S. M. C.; Parra, G.; Ross, E.; Moore, B.; Holt, C.; Sánchez Alvarado, A.; Yandell, M. *Genome Res.* **2008**, *18*, 188–196.
- (50) Smit, A. F. A.; Hubley, R.; Green, P. *RepeatMasker Open-4.0*; <http://www.repeatmasker.org>.
- (51) Price, A. L.; Jones, N. C.; Pevzner, P. A. *Bioinform.* **2005**, *21*, i351–i358.
- (52) Stanke, M.; Morgenstern, B. *Nucleic Acids Res.* **2005**, *33*, W465–W467.
- (53) Korf, I. *BMC Bioinform.* **2004**, *5*, 59.
- (54) Weber, T.; Blin, K.; Duddela, S.; Krug, D.; Kim, H. U.; Bruccoleri, R.; Lee, S. Y.; Fischbach, M. A.; Müller, R.; Wohlleben, W.; Breitling, R.; Takano, E.; Medema, M. H. *Nucleic Acids Res.* **2015**, *43*, W237–W243.
- (55) Khaldi, N.; Seifuddin, F. T.; Turner, G.; Haft, D.; Nierman, W. C.; Wolfe, K. H.; Fedorova, N. D. *Fungal Genet. Biol.* **2010**, *47*, 736–741.
- (56) Wattam, A. R.; Gabbard, J. L.; Shukla, M.; Sobral, B. W. *Methods Mol. Biol.* **2014**, *1197*, 287–308.
- (57) Eddy, S. R. *Genome Inform.* **2009**, *23*, 205–211.
- (58) Finn, R. D.; Clements, J.; Eddy, S. R. *Nucleic Acids Res.* **2011**, *39*, W29–W37.
- (59) Edgar, R. C. *Nucleic Acids Res.* **2004**, *32*, 1792–1797.
- (60) Mujic, A. B. Symbiosis in the Pacific Ring of Fire: Evolutionary Biology of Rhizopogon Subgenus Villosuli as Mutualists of Pseudotsuga. Ph.D. Dissertation, Oregon State University, Corvallis, OR, 2015.
- (61) Stamatakis, A. *Bioinformatics* **2006**, *22* (21), 2688–2690.
- (62) Aron, A. T.; Gentry, E. C.; McPhail, K. L.; Nothias, L.-F.; Nothias-Esposito, M.; Bouslimani, A.; Petras, D.; Gauglitz, J. M.; Sikora, N.; Vargas, F.; van der Hooft, J. J. J.; Ernst, M.; Kang, K. B.; Aceves, C. M.; Caraballo-Rodríguez, A. M.; Koester, I.; Weldon, K. C.; Bertrand, S.; Roullier, C.; Sun, K.; Tehan, R. M.; Boya P, C. A.; Christian, M. H.; Gutiérrez, M.; Ulloa, A. M.; Tejada Mora, J. A.; Mojica-Flores, R.; Lakey-Beitia, J.; Vázquez-Chaves, V.; Zhang, Y.; Calderón, A. I.; Tayler, N.; Keyzers, R. A.; Tugizimana, F.; Ndlovu, N.; Aksenov, A. A.; Jarmusch, A. K.; Schmid, R.; Truman, A. W.; Bandeira, N.; Wang, M.; Dorrestein, P. C. *Nat. Protoc.* **2020**, *15*, 1954–1991.
- (63) Yu, Q.; Ma, X.; Xu, L. *Thermochim. Acta* **2013**, *558*, 6–9.